Wood-Adhesive Bonding Failure: Modeling and Simulation

Zhiyong Cai
Project Leader, Forest Products Laboratory, USDA Forest Service, Madison, Wisconsin

Abstract

The mechanism of wood bonding failure when exposed to wet conditions or wet/dry cycles is not fully understood and the role of the resulting internal stresses exerted upon the wood-adhesive bondline has yet to be quantitatively determined. Unlike previous modeling this study has developed a new two-dimensional internal-stress model on the basis of the mechanics of layered composites. Plywood panel is regarded as a multi-layered composite material where each layer (including bonding line) has different properties. When the plywood panel experiences moisture changes through its thickness, internal stresses and their corresponding strains develop among its layers. The model can be used to quantitatively simulate the relationship between the internal stresses and the panel parameters which include layer thickness, modulus of elasticity, linear expansion coefficient, Poisson's ratio, shear modulus, density, and orientation of layers. The results may provide a better understanding of bonding failure during the water-exposure test. This paper describes the model development.

Background

Failure of wood bonding due to exposure to wet conditions or wet/dry cycles is a longstanding problem associated with development of acceptable wood adhesives in the plywood industries. Usually, the bonding performance needs to be evaluated through a water-soak test or test involving dramatic changes in moisture. The literature contains significant performance data, but understanding of how the changes in moisture influence the bonding process and failure mechanism is more limited (Frihart 2009). As explained by most research studies, moisture changes result in dimensional changes (expansion or shrinkage) in wood and glue. The difference in the dimensional changes along the bondline and adjacent wood layers induces internal stress between wood and bonding line. When the internal stress exceeds the bonding (or glue) strength, delamination or bonding failure occurs.

Many premises have been proposed to qualitatively explain the development of internal stresses due to the moisture changes. River et al. (1991) placed the emphasis on bond failure during the wood shrinkage stage as the wood lost moisture content. However, Gillespie (1976) and Frihart et al. (2008) considered that swelling of the wood under increasing moisture conditions could also lead to poor integrity of the bond and cause adhesive bonding failure.

Frihart (2009) searched the available literature and developed several qualitative models based on his research to help explain the results observed with different adhesives and different wood species under different test conditions. The first related to the importance of appreciating that the greater swelling of the wood compared to the adhesive leads to stress at the wood–adhesive interface. The second related to knowing whether the adhesive did or did not help to distribute this strain so as to reduce the interfacial stress.

To determine the failure location within the bondline for more adhesive systems, Marra (1992) separated the bonding region into nine domains/layers: both bulk wood (W), both wood interphases (W-I), both wood–adhesive interfaces (W-A), both adhesive interphases (A-I) and bulk adhesive (Adhesive). Considering this bondline structure, it is possible to regard it as a multi-layered composite material, where each layer has a unique set of physical properties. Individual layers can be approximated as an orthotropic material having two principle directions. Sun (1994) showed that the behavior of wood composites could be modeled using the mechanics of layered composites. The goal of this study is to investigate and model the mechanism of wood–adhesive bonding interfaces using the theory of mechanics of layered composites and thus provide insight into understanding the structure and performance of the bonding adhesion.

Introduction to Mechanics of Layered Composites

The mechanical behavior of layered composite materials is quite different from that of most common engineering materials which are homogeneous and isotropic.

Wood has unique and independent mechanical properties in the directions of three mutually perpendicular axes, so it may be described as an orthotropic material (Forest Products Laboratory 1999). The makeup and physical properties of layered composites varies with location and orientation of the principle axes. **Figure 1** shows a typical, thin wood veneer with two principle directions that are perpendicular to each other. For thin layers, a state of plane-stress parallel to the laminate can be assumed with reasonable accuracy. The two-dimensional stress-strain equation is (Sun 1994):

$$\begin{Bmatrix} \sigma_1 \\ \sigma_2 \\ \sigma_{12} \end{Bmatrix} = \begin{bmatrix} \frac{E_1}{1-\upsilon_{12}\ {}_{21}} & \frac{\upsilon_{12}E_2}{1-\upsilon_{12}\upsilon_{21}} & 0 \\ \frac{\upsilon_{12}E_2}{1-\upsilon_{12}\upsilon_{21}} & \frac{E_2}{1-\upsilon_{12}\upsilon_{21}} & 0 \\ 0 & 0 & G_{12} \end{bmatrix} \begin{Bmatrix} \varepsilon_1 \\ \varepsilon_2 \\ \gamma_{12} \end{Bmatrix} \qquad [1]$$

where 1 and 2 represent the two principle coordinate directions; E_1 and E_2 are the moduli of elasticity along the two directions; σ_{11} and σ_{22} are stresses along the two principle coordinates; σ_{12} is the in-plane shear stress; G_{12} is the in-plane shear modulus; υ_{12} is Poisson's ratio measuring contraction in the 1-direction due to uniaxial loading in the 2-direction; υ_{21} is Poisson's ratio measuring contraction in the 2-direction due to uniaxial loading in the 1-direction; ε_{11} and ε_{22} are strains along the two principle coordinates; and γ_{12} is the shear strain. The 3 × 3 matrix of elastic constants is usually denoted by:

$$[Q] = \begin{bmatrix} Q_{11} & Q_{12} & 0 \\ Q_{12} & Q_{22} & 0 \\ 0 & 0 & Q_{66} \end{bmatrix} \qquad [2]$$

Usually, during the construction of plywood, the grain orientation of each layer may be different. **Figure 2** shows an example of five-layer plywood. The principle grain directions of the second and fourth layers from the top are ±45° from the overall coordinate *x-y*, respectively. The product is called [0/45/90/–45/0] balanced construction. Therefore, in stress analysis, if a coordinate system, *x-y*, is set up which does not coincide with the material principle axes *1-2* (the right side of **Fig. 1**), the two sets of stress-strain components must be transformed to the two-coordinates system. The two-dimensional stress-strain equation in a global *x-y* system is then:

$$\begin{Bmatrix} \sigma_x \\ \sigma_y \\ \sigma_{xy} \end{Bmatrix} = [\bar{Q}] \begin{Bmatrix} \varepsilon_x \\ \varepsilon_y \\ \gamma_{xy} \end{Bmatrix} \qquad [3]$$

where:

$$[\bar{Q}] = \begin{bmatrix} \cos^2\theta & \sin^2\theta & 2\sin\theta\cos\theta \\ \sin^2\theta & \cos^2\theta & -2\sin\theta\cos\theta \\ -\sin\theta\cos\theta & \sin\theta\cos\theta & \cos^2\theta - \sin^2\theta \end{bmatrix}^{-1} [Q] \begin{bmatrix} \cos^2\theta & \sin^2\theta & \sin\theta\cos\theta \\ \sin^2\theta & \cos^2\theta & -\sin\theta\cos\theta \\ -2\sin\theta\cos\theta & 2\sin\theta\cos\theta & \cos^2\theta - \sin^2\theta \end{bmatrix} \qquad [4]$$

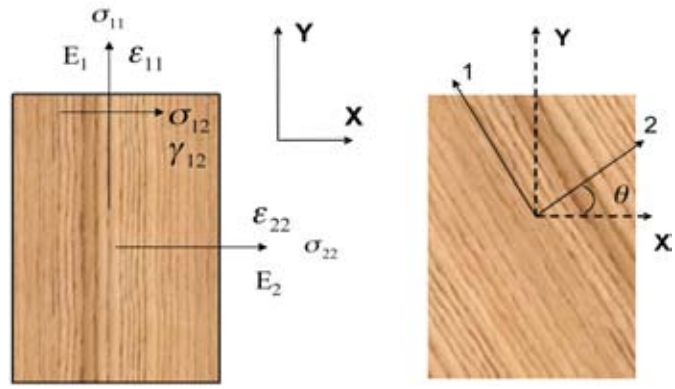

Figure 1. ~ *Orthotropic characteristics of thin layer veneer and its coordinates.*

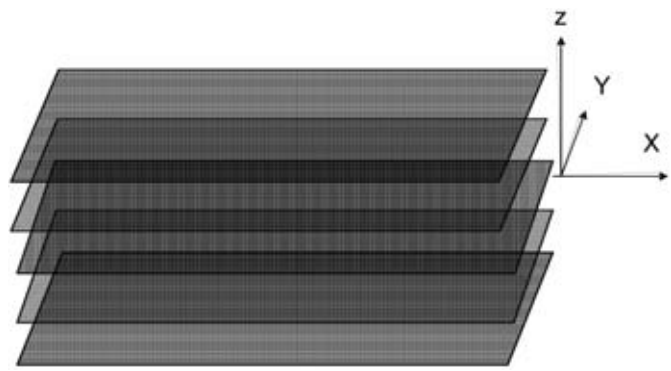

Figure 2. ~ *An example of a five-layer composite with different orientations.*

A layered composite consists of a number of laminae with different orintations in the thickness direction (**Fig. 2**). To establish a constitutive equation for the composite, the stress and strain components of each layer must be transformed to the global *x-y* coordinates for the composite. For a uniform composite plate with thickness of *h*, the plate resultant forces {*N*} and moments {*M*} are defined by:

$$\begin{Bmatrix} N_x \\ N_y \\ N_{xx} \end{Bmatrix} = \int_{-h/2}^{h/2} \begin{Bmatrix} \sigma_x \\ \sigma_y \\ \sigma_{xy} \end{Bmatrix} dz \qquad [5]$$

and

$$\begin{Bmatrix} M_x \\ M_y \\ M_{xx} \end{Bmatrix} = \int_{-h/2}^{h/2} \begin{Bmatrix} \sigma_x \\ \sigma_y \\ \sigma_{xy} \end{Bmatrix} z dz \qquad [6]$$

where *z* is in the thickness direction. When a composite plate consists of *n* thin layers where each layer

has different properties, the plate resultant forces and moments will be summations of resultant forces and moments of each layer, respectively. Assuming the ith layer located at thickness region from $z = z_{i-1}$ to $z = z_i$, the plate resultant forces and moments of a composite with n layers will become:

$$\begin{Bmatrix} N_x \\ N_y \\ N_{xx} \end{Bmatrix} = \sum_{i=1}^{n} \int_{z_{i-1}}^{z_i} \begin{Bmatrix} \sigma_x \\ \sigma_y \\ \sigma_{xy} \end{Bmatrix}_i dz \qquad [7]$$

and

$$\begin{Bmatrix} M_x \\ M_y \\ M_{xx} \end{Bmatrix} = \sum_{i=1}^{n} \int_{z_{i-1}}^{z_i} \begin{Bmatrix} \sigma_x \\ \sigma_y \\ \sigma_{xy} \end{Bmatrix}_i zdz \qquad [8]$$

Equation [3] describes the relationship between stresses and strains in the global x-y coordinate for the laminate. Due to the plate resultant forces and moments that could be caused by unbalanced internal stresses from different expansions or shrinkages of each layer, the strains in the laminate include two major components. One is the in-plane strain including ε^0_x, ε^0_y, and γ^0_{xy}. The other is out-plane strain due to the bending with the curvatures of κ_x, κ_y, and κ_{xy}. The **Eq.** [3] is then:

$$\begin{Bmatrix} \sigma_x \\ \sigma_y \\ \sigma_{xy} \end{Bmatrix} = [\bar{Q}] \left(\begin{Bmatrix} \varepsilon^0_x \\ \varepsilon^0_y \\ \varepsilon^0_{xy} \end{Bmatrix} + z \begin{Bmatrix} \kappa_x \\ \kappa_y \\ \kappa_{xy} \end{Bmatrix} \right) \qquad [9]$$

Substituting **Eq.** [9] to **Eqs.** [7] and [8], we obtain:

$$\begin{Bmatrix} N_x \\ N_y \\ N_{xx} \end{Bmatrix} = \sum_{i=1}^{n} [\bar{Q}]_i \left(\int_{z_{i-1}}^{z_i} \begin{Bmatrix} \varepsilon^0_x \\ \varepsilon^0_y \\ \varepsilon^0_{xy} \end{Bmatrix}_i dz + \int_{z_{i-1}}^{z_i} \begin{Bmatrix} \kappa_x \\ \kappa_y \\ \kappa_{xy} \end{Bmatrix} zdz \right) \qquad [10]$$

and

$$\begin{Bmatrix} M_x \\ M_y \\ M_{xx} \end{Bmatrix} = \sum_{i=1}^{n} [\bar{Q}]_i \left(\int_{z_{i-1}}^{z_i} \begin{Bmatrix} \varepsilon^0_x \\ \varepsilon^0_y \\ \varepsilon^0_{xy} \end{Bmatrix}_i zdz + \int_{z_{i-1}}^{z_i} \begin{Bmatrix} \kappa_x \\ \kappa_y \\ \kappa_{xy} \end{Bmatrix} z^2 dz \right) \qquad [11]$$

Since both in-plane and out-of-plane strains are independent of z, the integration in **Eqs.** [10] and [11] can be performed. The results can be combined into the following form, which is the constitutive equation for the composite:

$$\begin{Bmatrix} N_x \\ N_y \\ N_{xy} \\ M_x \\ M_y \\ M_{xy} \end{Bmatrix} = \begin{bmatrix} A_{11} & A_{12} & A_{16} & B_{11} & B_{12} & B_{16} \\ A_{12} & A_{22} & A_{26} & B_{11} & B_{22} & B_{26} \\ A_{16} & A_{26} & A_{66} & B_{16} & B_{26} & B_{66} \\ B_{11} & B_{12} & B_{16} & D_{11} & D_{12} & D_{16} \\ B_{12} & B_{22} & B_{26} & D_{12} & D_{22} & D_{26} \\ B_{16} & B_{26} & B_{66} & D_{16} & D_{26} & D_{66} \end{bmatrix} \begin{Bmatrix} \varepsilon^0_x \\ \varepsilon^0_y \\ \gamma^0_{xy} \\ \kappa^0_x \\ \kappa^0_y \\ \kappa^0_{xy} \end{Bmatrix} \qquad [12]$$

In addition to the external stresses (i.e., self-weight or restraint), wood composites sometimes have experienced significant internal stresses due to thermal changes (superscript T) and moisture movements (superscript H). Including the internal stresses, **Eq.** [12] becomes:

$$\begin{Bmatrix} N_x \\ N_y \\ N_{xy} \\ M_x \\ M_y \\ M_{xy} \end{Bmatrix} + \begin{Bmatrix} N^T_x \\ N^T_y \\ N^T_{xy} \\ M^T_x \\ M^T_y \\ M^T_{xy} \end{Bmatrix} + \begin{Bmatrix} N^H_x \\ N^H_y \\ N^H_{xy} \\ M^H_x \\ M^H_y \\ M^H_{xy} \end{Bmatrix} = \begin{bmatrix} A_{11} & A_{12} & A_{16} & B_{11} & B_{12} & B_{16} \\ A_{12} & A_{22} & A_{26} & B_{11} & B_{22} & B_{26} \\ A_{16} & A_{26} & A_{66} & B_{16} & B_{26} & B_{66} \\ B_{11} & B_{12} & B_{16} & D_{11} & D_{12} & D_{16} \\ B_{12} & B_{22} & B_{26} & D_{12} & D_{22} & D_{26} \\ B_{16} & B_{26} & B_{66} & D_{16} & D_{26} & D_{66} \end{bmatrix} \begin{Bmatrix} \varepsilon^0_x \\ \varepsilon^0_y \\ \gamma^0_{xy} \\ \kappa^0_x \\ \kappa^0_y \\ \kappa^0_{xy} \end{Bmatrix} \qquad [13]$$

Symbolically, **Eq.** [13] is expressed in the following form:

$$\begin{Bmatrix} N \\ M \end{Bmatrix} + \begin{Bmatrix} N^T \\ M^T \end{Bmatrix} + \begin{Bmatrix} N^H \\ M^H \end{Bmatrix} = \begin{bmatrix} A & B \\ B & D \end{bmatrix} \begin{Bmatrix} \varepsilon^0 \\ \kappa^0 \end{Bmatrix} \qquad [14]$$

where $\{N\}$ are the plate resultant external forces; $\{M\}$ are the plate resultant external moments; $\{\varepsilon^0\}$ are the in-plane strains; $\{\kappa^0\}$ are the curvatures of the mid-surface, and

$$A_{jk} = \sum_{i=1}^{n} \bar{Q}^{(i)}_{jk} t_i \qquad [15]$$

$$B_{jk} = \sum_{i=1}^{n} \bar{Q}^{(i)}_{jk} t_i z_i \qquad [16]$$

$$D_{jk} = \sum_{i=1}^{n} \bar{Q}^{(i)}_{jk} \left(t_i z_i^2 + \frac{t_i^3}{12} \right) \qquad [17]$$

$$\{N^T\} = \Delta T \sum_{i=1}^{n} [\bar{Q}]_i \{\alpha^T\}_i t_i \qquad [18]$$

$$\{M^T\} = \Delta T \sum_{i=1}^{n} [\bar{Q}]_i \{\alpha^T\}_i t_i z_i \qquad [19]$$

$$\{N^H\} = \Delta H \sum_{i=1}^{n} [\bar{Q}]_i \{\alpha^H\}_i t_t \qquad [20]$$

$$\{M^H\} = \Delta H \sum_{i=1}^{n} [\bar{Q}]_k \{\alpha^H\}_i t_i z_i \qquad [21]$$

where t_i is the thickness of the ith layer; z_i is the centroid of the ith layer; $\{N^T\}$ and $\{M^T\}$ are the plate internal forces and moments due to change of temperature (ΔT) at thermal expansion coefficient of $\{\alpha^T\}$; $\{N^H\}$ and $\{M^H\}$ are the plate internal forces and moments due to change of moisture content (ΔH) at linear expansion coefficient of $\{\alpha^H\}$.

For most wood composite panels, deformation or dimensional changes are mainly caused by moisture movement. For free hygroscopical expansion where there is no external stresses and thermal stresses ($\{N\}=\{M\}=\{N^T\}=\{N^T\}=\{0\}$), **Eq.** [14] then becomes:

$$\begin{Bmatrix} N^H \\ M^H \end{Bmatrix} = \begin{bmatrix} A & B \\ B & D \end{bmatrix} \begin{Bmatrix} \varepsilon^0 \\ \kappa^0 \end{Bmatrix} \qquad [22]$$

After knowing the internal stress distribution within each layer, it is simple to determine the failure mode inside the bonding line. There are a few failure criteria available in the literature. Among them the most popular one is the Hill-Tsai failure criterion (Hill 1950 and Tsai 1965) [**Eq. 23**]. For an orthotropic lamina, the stress level (SL) is determined by considering the combined

stresses in two principle directions. If SL is greater than or equal to 100%, then the lamina ruptures.

$$SL = \left[\frac{\sigma_{11}}{T_1}\right]^2 + \left[\frac{\sigma_{22}}{T_2}\right]^2 - \left[\frac{\sigma_{11}}{T_1}\right]\left[\frac{\sigma_{22}}{T_2}\right] + \left[\frac{\sigma_{12}}{S}\right] \qquad [23]$$

where σ_{11} and σ_{22} are stresses along the two principle coordinates; σ_{12} is the in-plane shear stress; T_1 and T_2 are the tension strengths in two directions; and S is the in-plan shear strength.

Computer Program and Modeling

Using Microsoft Excel, Cai and Dickens (2004) developed a computer program on the theory and mechanism described above. Wood-adhesive bonding interfaces are modeled as composites consisting of nine layers with different orientations and properties. Once the model has been given input parameters (**Table 1**), it will calculate and plot the internal stress occurring on the bonding line (shown in **Fig. 3**) at the free boundary conditions. The input parameters include the following information for each layer: MOE in the two principle coordinate directions; layer orientation (θ); Poisson's ratios; thickness; linear expansion coefficient due to MC changes; thermal expansion coefficients; change in MC; change in temperature; shear modulus; tensile strengths in two principle directions.

The input parameters in **Table 1** purposely simulate the moisture penetrating from the top faces only. The moisture content of the first layer from the top is 4%, and 3% for the second layer, 2% for the third layer, and 1% for the fourth layer. The moisture content of the bottom layers remains unchanged (0%). As soon as the moisture moves into the top layers, their dimensions expand. This generates unbalanced stresses inside the laminate, specifically, compression stresses among the top layers and tensile stresses within the bottom layers. The stress level is determined by considering the combined stresses and their strengths in two principle directions [**Eq. 23**]

Table 1. ~ *Estimated properties of each layer adjusted to the wood-adhesive bondline.*

Layers†	Thickness	E_1‡	E_2‡	V_{12}§	LEC_1¶	LEC_2¶	ΔMC#	T_1††	T_2††46
	(mm)	(GPa)	(GPa)		mm/mm %MC	mm/mm %MC	%	(MPa)	(MPa)
W	2.540	12.62	0.63	0.400	6.000E-04	1.600E-03	4.0	23.10	2.41
W-I	0.400	12.62	0.63	0.400	6.000E-04	1.600E-03	3.0	23.10	2.41
W-A	0.030	12.62	0.63	0.400	6.000E-04	1.600E-03	2.0	23.10	2.41
A-I	0.003	6.89	0.34	0.250	6.000E-04	1.600E-03	1.0	23.10	2.41
Adhesive	0.003	3.45	3.45	0.250	4.000E-04	4.000E-04	0.0	34.47	34.47
A-I	0.003	6.89	0.34	0.250	6.000E-04	1.600E-03	0.0	23.10	2.41
W-A	0.030	12.62	0.63	0.400	6.000E-04	1.600E-03	0.0	23.10	2.41
W-I	0.400	12.62	0.63	0.400	6.000E-04	1.600E-03	0.0	23.10	2.41
W	2.540	12.62	0.63	0.400	6.000E-04	1.600E-03	0.0	23.10	2.41

†Different layers: W = wood, W-I = wood interface, W-A = wood with impregnated adhesive, A-I = adhesive interface.

‡E_1 is modulus of elasticity in grain direction and E_2 is perpendicular to the grain direction.

§V_{12} = Poisson ratio.

¶LEC_1 = linear expansion coefficient in grain direction and LEC_2 is perpendicular to the grain direction.

#MC = Change of moisture content; LEC = linear expansion coefficient.

††T_1 is tension strength in grain direction and T_2 is perpendicular to the grain direction.

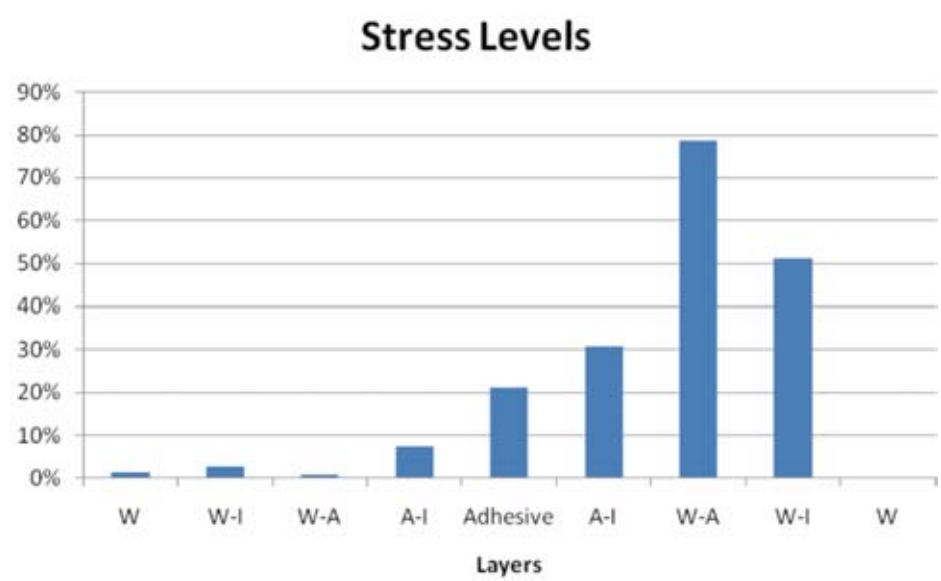

Figure 3. ~ *Simulated stress level (SL), calculated from Eq. 23, within each layer based on the data in Table 1.*

is used to describe the stress distribution (**Fig. 3**). If SL within a lamina is greater than or equal to 100%, then the lamina ruptures. Since the compression strength of wood is much greater than the tensile strengths, the SL due to the compression stresses is usually much lower than the one caused by the tensile stresses. That's why there is an unbalanced distribution of SL in **Fig. 3**. If the composite has symmetrical lamination and moisture variations, the stress level distribution within the composite will be symmetrical as well.

Given the many parameters that affect internal stress distribution, most researchers focus on the effects of moisture gradient and resin-bonding performance. It is impossible for researchers to design an experiment to investigate all possible parameter effects on internal stresses, since these parameters are interactive. Therefore, to provide a better understanding of adhesive bonding failure, it is necessary to simulate all possible parameter effects on bonding performance in the newly developed computer model.

To better simulate the bonding performance, the accurate information of the properties of each layer around the adhesive bonding line is critical. **Table 1** only contains the data obtained from Wood Handbook (Forest Products Laboratory 1999), previous study (Cetin and Ozmen 2003), and personal contacts. On the basis of the data in **Table 1**, the computer model provides the internal stress distribution in each layer. A project has been designed and is underway to accurately characterize the layers using nano-indentation and x-ray densitometer. The result may help to provide better understanding of adhesive bonding performance through dramatic moisture change.

Summary

Adhesive bonding performance between wood materials under the influence of a moisture gradient is modeled as a layered composite material. The adhesive bonding surface was divided into nine domains/layers: both bulk wood, both wood interfaces, both wood-adhesive interfaces, both adhesive interfaces, and bulk adhesive. The bonding interfaces can be regarded as a multi-layered composite material, where each layer has a unique set of physical properties. Mechanics of layered composites was used to investigate the internal stress distribution and a computer model was developed. After providing information about each layer regarding its properties and moisture movement, the new model calculated the corresponding internal stress level. Simulation of all possible parameter effects on the adhesive bonding performance in the newly developed computer model could provide a better understanding of the mechanism of adhesive-bonding failure during the water-exposure test.

Literature Cited

Cai, Z., and J.R. Dickens. 2004. Wood composite warping: Modeling and simulation. Wood Fiber Sci. 36(2):174–185.

Cetin, N.S., and N. Ozmen. 2003. Studies on lignin-based adhesives for particleboard panels. Turk. J. Agric. For. 27:183–189.

Forest Products Laboratory. 1999. Wood Handbook—Wood as an Engineering Material. Gen. Tech. Rep. FPL-GTR-113. U.S. Department of Agriculture, Forest Service, Forest Products Laboratory, Madison, WI.

Frihart, C.R. 2009. Adhesive classes and how they relate to the durability of bonded wood. J. Adhes. Sci. Technol. 23:601–617.

Frihart, C.R., D.J. Yelle, and A.C. Wiedenhoeft. 2008. *In* E 34 Final Workshop on Bonding of Timber, Sopron, Hungary.

Gillespie, R.H. 1976. Effect of internal stresses on bond strength of wood joints. Prepared for the Department of Housing & Urban Development, under agreement no. IAA-H-71, Amendment no. 1 on Adhesives. Washington, D.C.

Hill, R. 1950. Mathematical Theory of Plasticity. Oxford University Press, New York.

Marra, A.A. 1992. Technology of Wood Bonding: Principles in Practice. Van Nostrand Reinhold, New York.

River, B.H., C.B. Vick, and R.H. Gillespie. 1991. Treatise on Adhesion and Adhesives. Vol. 7, pp. 1–230. *In* J.D. Minford (ed.) Marcel Dekker, New York.

Sun, C.T. 1994. Mechanics of composite materials and laminates. Lecture notes for AAE 555. School of Aeronautics and Astronautics, Purdue University, West Lafayette, IN.

Tsai, S.W. 1965. Strength Characteristics of Composite Materials. NASA CR-224. Washington, D.C.

Wood Adhesives 2009 / edited by Charles R. Frihart, Chiristopher G. Hunt, and Robert J. Moon.
Madison, WI : Forest Products Society, c2010. 1 CD-ROM.
ISBN 978-1-892529-57-2. FPS Proceedings no. 7216-09.